Time-Dependent Wave Packet Split Operator Calculations on a Three-Dimensional Fourier Grid in Radau Coordinates Applied to the OClO Photoelectron Spectrum

Zhigang Sun[†] **and Nanquan Lou**

State Key Laboratory of Molecular Reaction Dynamics, Dalian Institute of Chemical Physics, Chinese Academy of Sciences, Dalian 116023, P. R. China

Gunnar Nyman*

Department of Chemistry, Physical Chemistry, Göteborg University, SE-412 96 Göteborg, Sweden

Received: May 26, 2004; In Final Form: August 9, 2004

A transformed Hamiltonian for a triatomic molecule in Radau coordinates is employed for time-dependent wave packet calculations. The first photoelectron band of the OClO molecule is calculated by propagating the wave packet on a three-dimensional Fourier grid with the split operator method. To find the intial wave function, we first calculate the few lowest one-dimensional eigenfunctions along each Radau coordinate by the Fourier grid Hamiltonian method. The direct product of these eigenfunctions is then used as basis set for obtaining the initial ground state vibrational wave function, which in this way is expressed directly on the three-dimensional Fourier grid. Consistent with the results of a previous two-dimensional study, we find that the asymmetric stretch plays little role in the photoionization process. An improved equilibrium geometry for the potential energy surface function of the ground electronic state of $OClO^+$ was found by iteratively comparing with the experimental photoelectron spectrum. Using the approach employed here, it is easy to treat a time-dependent Hamiltonian.

I. Introduction

Modern techniques to solve the time-dependent Schrödinger equation play an important role in the description of atomic and molecular processes.[1−7] In many realistic molecular calculations, the numerical method is often to first solve the electronic structure problem to produce a set of potential energy surfaces and then to consider the nuclear motion quantum dynamically. As the computational time increases exponentially with the number of degrees of freedom of the system, it is necessary to consider which coordinate system to employ. This usually means working in a body fixed frame, but there does not seem to exist a special coordinate system with general advantages for every problem and system of interest. Katz et al.[8] found in a comparative study at most a factor of 3 difference in computer time between calculations employing four different coordinate systems, once the grid parameters had been optimized using a phase space criteria.[8] There are, however, some general considerations which are helpful in choosing the coordinates for the system of interest. For instance, hyperspherical coordinate systems, which employ only one radial coordinate to describe all arrangement channels, can reduce the number of grid points required in studying chemical reactions or molecular dissociations.[9] Using Jacobi coordinates for describing the dynamics of atom−diatom van der Waals complexes and triatomic molecules having one atom much lighter than the other two[10] may be advantageous.

Among the common body-fixed coordinates describing triatomic molecules, Eckart bond coordinates are advantageous for visualizing the nuclear motion.[8] However the triatomic Hamiltonian of a molecule in Eckart bond coordinates is complex, and it requires many forward and backward Fourier transforms if such are used in a wave packet propagation.[8] Thus, the numerical efficiency is lower than if Jacobi coordinates are used, where the evaluation of the Laplacian operator only requires three forward−backward Fourier transforms. However, there exists a set of coordinates named after Radau[11−15] in which the time-dependent wave packet for a triatomic molecule resembles the motion in Eckart bond coordinates, particularly if the central atom is heavy. Conveniently, the triatomic Hamiltonian in Radau coordinates is identical in form to that in Jacobi coordinates.[16,17] Thus, only three Fourier transforms are required to propagate the wave packet one time step in Radau coordinates.

An attractive aspect of the time-dependent wave packet method is that much insight can be obtained by inspecting snapshots of the wave packet at regular time intervals. From the snapshots of the wave packet in Radau coordinates it is easy to visualize the nuclear motion because of the resemblance between the Radau and Eckart bond coordinates. This aspect may be of special interest in real time studies of pump−probe experiments. In this work we employ Radau coordinates to calculate the first band of the He I photoelectron spectrum of OClO.

The paper is arranged as follows: Section II contains theory. It first revisits the triatomic Hamiltonian in Radau coordinates. Then it is explained how the initial vibrational ground state wave function is obtained and how the wave packet is propagated on a three-dimensional Fourier grid using the split-operator method. Further, some details on the calculation of the photoelectron spectrum, the potential energy surfaces and the numerical parameters are given. In section III, the results are presented and discussed. A brief investigation of the numerical performance for calculating the vibrational eigenenergies of OClO is

[†] The work was performed during a visit to Göteborg University. E-mail: zsun@dicp.ac.cn.

10.1021/jp0477203 CCC: $27.50
Published on Web 09/22/2004

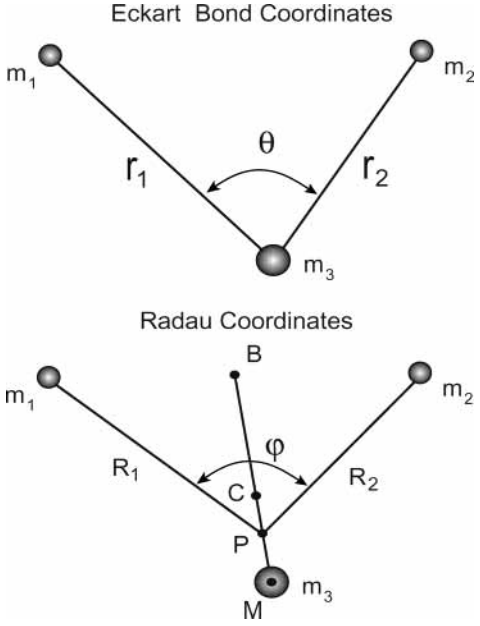

Figure 1. Triatomic Radau (R_1, R_2, φ) and Eckart bond (r_1, r_2, θ) coordinates. For OClO, m_1 and m_2 are the oxygen atoms and m_3 the chlorine atom. Point B is the center of mass of the two oxygen atoms, C is the triatomic center of mass, and P is a canonical point satisfying the condition $\overline{MB} \times \overline{CB} = \overline{PB}^2$.

presented together with the calculated first photoelectron band of the OClO molecule. Finally an improved equilibrium geometry for the ground electronic state of $OClO^+$ is put forth. We summarize our findings in section IV.

II. Theoretical Method

A. Triatomic Hamiltonian in Radau Coordinates. The traditional Radau coordinates of a triatomic molecule are shown in Figure 1. R_1, R_2, and φ constitute the Radau coordinates, which resemble r_1, r_2, and θ, the bond lengths and the bond angle in Eckart bond coordinates. For completeness, a brief description for setting up Radau coordinates is given here. In Figure 1, point C is the triatomic center of mass, and for OClO point B is the center of mass of the two nonbonded oxygen atoms. Point P is one of the canonical points.[15] As measured from B, the distance to P is the geometric mean of the distance to M and C, that is, $\overline{MB} \times \overline{CB} = \overline{PB}^2$. For OClO, M indicates the position of the chlorine atom. Although point P depends on the values of the bond lengths and the bond angle, it varies little when the central atom is heavy. Therefore, for some triatomic systems we approximately obtain the nuclear motion in Eckart bond coordinates from snapshots of the time-dependent wave packet even if it is represented in Radau coordinates. We note that the OClO molecule has a relatively heavy central atom.

The Hamiltonian in Radau coordinates for a nonrotating triatomic molecule in atomic units is[14]

$$\hat{H} = -\frac{1}{2m_1}\frac{\partial^2}{\partial {R_1}^2} - \frac{1}{2m_2}\frac{\partial^2}{\partial {R_2}^2} - \frac{1}{2}\left(\frac{1}{m_1 {R_1}^2} + \frac{1}{m_2 {R_2}^2}\right)\frac{1}{\sin\varphi}\frac{\partial}{\partial\varphi}\sin\varphi\frac{\partial}{\partial\varphi} + V(R_1,R_2,\varphi,t) \quad (1)$$

We note that for the OClO molecule, setting the total angular momentum $J = 0$ is an approximation, even at zero temperature, as the ro-vibrational ground state has an angular momentum of $J = {}^1/_2$.

In the numerical implementation a transformed form of the Hamiltonian in eq 1 is used. It is obtained by setting $\Psi(R_1,R_2,\varphi) = \Phi(R_1,R_2,\varphi)\ \sin^{-1/2}\varphi$[18], where Φ is the wave function for eq 1. The new Hamiltonian is

$$\hat{\mathrm{H}} = -\frac{1}{2m_1}\frac{\partial^2}{\partial {R_1}^2} - \frac{1}{2m_2}\frac{\partial^2}{\partial {R_2}^2} - \frac{1}{2}\left(\frac{1}{m_1 {R_1}^2} + \frac{1}{m_2 {R_2}^2}\right)\left(\frac{\partial^2}{\partial\varphi^2} + \frac{1}{4\sin^2\varphi} + \frac{1}{4}\right) + V(R_1,R_2,\varphi,t) \quad (2)$$

The volume element for $\hat{\mathrm{H}}$ in eq 2 is $\alpha^{-3}\ \mathrm{d}R_1\ \mathrm{d}R_2\ \mathrm{d}\varphi$, where $\alpha^2 = m_3/(m_1 + m_2 + m_3)$. m_1 and m_2 are the masses of the two oxygen atoms, and m_3 is the mass of the chlorine atom. This transformed Hamiltonian has singularities at $\varphi = 0$ and $\varphi = \pi$. Special attention must be paid to this when using the Hamiltonian for cases where collinear geometries occur. By the transformation, the mixture of local and nonlocal operators of the same coordinate disappears, which otherwise prohibits the use of the split-operator method for propagating the wave packet.[19] For cases where collinear geometries occur, a useful Hamiltonian is obtained by a change of variable from φ to $\cos\varphi$ in the Hamiltonian in eq 1. However, the grid then becomes equidistant in the variable $\cos\varphi$ rather than in φ. Further, the split-operator method cannot be used to propagate the wave packet.

Often the potential energy surfaces of triatomic molecules are expressed in Eckart bond coordinates. The relationship between Radau (R_1,R_2,φ) and Eckart bond (r_1,r_2,θ) coordinates can be written as

$$R_1 = \sqrt{(1+a)^2 {r_1}^2 + b^2 {r_2}^2 + 2(1+a)b r_1 r_2 \cos\theta} \quad (3)$$

$$R_2 = \sqrt{(1+b)^2 {r_2}^2 + a^2 {r_1}^2 + 2(1+b)a r_1 r_2 \cos\theta} \quad (4)$$

$$\cos\varphi = ({R_1}^2 + {R_2}^2 - {r_1}^2 - {r_2}^2 + 2r_1 r_2 \cos\theta)/(2R_1R_2) \quad (5)$$

where $a = (\alpha - 1)m_1/(m_1 + m_2)$ and $b = (\alpha - 1)m_2/(m_1 + m_2)$. The Jacobian factors wrt to Cartesian coordinates are $\alpha^{-3}R_1^2R_2^2\sin\varphi\ \mathrm{d}R_1\ \mathrm{d}R_2\ \mathrm{d}\varphi$ and $r_1^2r_2^2\sin\theta\ \mathrm{d}r_1\ \mathrm{d}r_2\ \mathrm{d}\theta$ for the Radau and Eckart bond coordinates respectively, which is useful in transforming between these coordinate systems.

B. The Initial Wave Function. Before propagating the wave packet, its initial form has to be defined. For the current calculation of a photoelectron spectrum, we need the lowest vibrational eigenfunction of the ground electronic state of the neutral OClO molecule, in which most of the population initially resides. Here we introduce a method for finding the initial wave packet on a three-dimensional Fourier grid, which is based on the Fourier grid Hamiltonian method[20,21] and resembles the method used by Füsti-Molnár et al.[10] for finding eigenvalues of the HOBr molecule.

To obtain one-dimensional basis functions for each of the body-fixed variables, R_1, R_2 and φ, we use the 1-dimensional Fourier grid Hamiltonian (FGH) method of Marston and Balint-Kurti[20] for finding diatomic vibrational eigenfunctions. This is done by varying one variable and fixing the other two at their equilibrium values. The resulting Hamiltonian matrix is then diagonalized in a one-dimensional Fourier grid basis. In this way, we obtain three sets of eigenfunctions, one set for each of the three variables. The number of eigenfunctions kept in each set is truncated before the direct product of them is formed and used as the basis set for solving the complete three-dimensional

problem. When calculating the Hamiltonian matrix for this basis set, the actions of the kinetic energy operators can be realized by utilizing three one-dimensional transformation matrices from the space coordinates to momentum coordinates,[20] or by the fast Fourier transform technique.[21] For both of these alternatives, we find that the diagonalization procedure used here is efficient for the current study of the OClO molecule. For simplicity we refer to the three-dimensional FGH method now described as the 3D FGH method. We also note that the one-dimensional potential cuts are helpful for deciding the grid ranges to be used in the calculations.

C. Time Evolution Operators. To accurately and effectively calculate the action of the operators of the Hamiltonian on the wave packet, a DVR grid,[22] or Lagrange mesh,[23] is often used.[24−26] Recently, it has been shown that the Fourier grid Hamiltonian method essentially is a special case of a Lagrange mesh calculation in which the kinetic energy operator is treated by a discrete Fourier transform.[27] That is, according to the nomenclature of the DVR method, the transformation of the grid or DVR basis function to the finite basis representation is done using discrete Fourier transformation and the grid points are evenly distributed. The Fourier grid Hamiltonian method is developed from physical insight,[1,20] but has a firm mathematical basis.[22−27] The FGH was developed to solve eigenenergy problems. It is numerically fast and easy to apply a discrete fast Fourier transform for realizing the action of the time evolution operator on the grid wave function and thus evolve the studied system in time.

The Hamiltonian in eq 2 can be rewritten as

$$\hat{H} = \hat{T}_{R_1} + \hat{T}_{R_2} + \hat{T}_{\varphi} + \hat{U}_{\mathrm{pot}}(R_1,R_2,\varphi,t) = -\frac{1}{2m_1}\frac{\partial^2}{\partial {R_1}^2} - \frac{1}{2m_2}\frac{\partial^2}{\partial {R_2}^2} - \frac{1}{2}\left(\frac{1}{m_1 {R_1}^2} + \frac{1}{m_2 {R_2}^2}\right)\frac{\partial^2}{\partial \varphi^2} + \Delta V + V(R_1,R_2,\varphi,t) \quad (6)$$

where the two last terms define the operator $\hat{U}_{\mathrm{pot}}(R_1,R_2,\varphi,t)$ and

$$\Delta V = -\frac{1}{2}\left(\frac{1}{m_1 {R_1}^2} + \frac{1}{m_2 {R_2}^2}\right)\left(\frac{1}{4\sin^2\varphi} + \frac{1}{4}\right) \quad (7)$$

In order to study dynamics, the time-dependent Schrödinger equation

$$i\frac{\partial}{\partial t}\Psi(R_1,R_2,\varphi,t) = [\hat{T}_{R_1} + \hat{T}_{R_2} + \hat{T}_{\varphi} + \hat{U}_{\mathrm{pot}}(R_1,R_2,\varphi,t)] \times \Psi(R_1,R_2,\varphi,t) \quad (8)$$

may be solved. The formal solution of the equation is

$$\Psi(R_1,R_2,\varphi,t) = \hat{U}(R_1,R_2,\varphi,t,t_0)\Psi(t_0) = \exp\left(-i\int_{t_0}^{t}[\hat{T}_{R_1} + \hat{T}_{R_2} + \hat{T}_{\varphi} + \hat{U}_{\mathrm{pot}}(R_1,R_2,\varphi,t')]\,\mathrm{d}t'\right) \times \Psi(R_1,R_2,\varphi,t_0) \quad (9)$$

To apply the short time split-operator method to propagate the initial wave function, the time is divided into N intervals in each of which the Hamiltonian changes little. The evolution operator can then be expressed as

$$\hat{U}(R_1,R_2,\varphi,t,t_0) = \prod_{n=0}^{N-1}\hat{\cup}(R_1,R_2,\varphi,(n+1)\Delta t + t_0, n\Delta t + t_0) \quad (10)$$

To evaluate the action of the time evolution operator on the wave function, the split-operator method is applied[19,28,29]

$$\hat{\cup}(R_1,R_2,\varphi,\Delta t,0) = \exp\{-i\Delta t[\hat{T}_{R_1} + \hat{T}_{R_2} + \hat{T}_{\varphi} + \hat{U}_{\mathrm{pot}}(R_1,R_2,\varphi,\Delta t/2)]\} \approx \exp(-i\Delta t\hat{T}_{R_1}/2)\exp(-i\Delta t\hat{T}_{R_2}/2)\exp(-i\Delta t T_{\varphi}/2) \times \exp\lfloor -i\Delta t\hat{U}_{\mathrm{pot}}(R_1,R_2,\varphi,\Delta t/2)\rfloor \times \exp(-i\Delta t\hat{T}_{\varphi}/2) \times \exp(-i\Delta t\hat{T}_{R_2}/2)\exp(-i\Delta t\hat{T}_{R_1}/2) \quad (11)$$

which gives correct terms up to second order on expanding the exponentials. Applying the operator $\hat{\cup}(R_1,R_2,\varphi,\Delta t,0)$ in eq 11 repeatedly, the last exponent in eq 11 can be merged with the first one.[28] Effectively, we thus get a product of six operators in each time step.

The five kinetic energy operators are nonlocal in coordinate space and are evaluated by fast Fourier transform. For each of them the second derivative is found keeping the other two coordinates fixed. The potential operator, which is local in coordinate space, acts in coordinate space. When the Fourier transform method is combined with the split-operator technique to propagate the initial wave packet, nonlocal and local operators of the same coordinate must not appear within a single term in the Hamiltonian.[19] This is one reason for using the transformed Radau Hamiltonian in eq 2.

Utilization of the split-operator method together with fast Fourier transform in the three-dimensional propagation allows for a highly efficient computer code and easy inclusion of effects of a time dependent external field. This is useful for studying ultrashort laser pulse interaction with molecules which is of current interest, particularly in coherent control involving shaped laser pulses.[5,6] We notice the similarity of the triatomic Hamiltonian in Jacobi coordinates with those in eqs 1 and 2, and thus how easily the computer code is adapted to Jacobi coordinates.

D. Photoelectron Spectrum. To calculate a photoelectron spectrum using the time-dependent wave packet approach, we first obtain the vibrational ground state wave function of the ground electronic state of the neutral OClO molecule. Then this wave function is vertically shifted to the potential energy surface of the ground electronic state of the cation,[31] where it is propagated. Finally the photoelectron spectrum is obtained as the Fourier transform of the wave function autocorrelation function.

The Fourier transform of the autocorrelation function can be written[31]

$$I(E) \propto |R_E|^2 \mathrm{Re}\int_0^{\infty} \mathrm{e}^{i(E+E_0)t} C'(t)\,\mathrm{d}t \quad (12)$$

where R_E is the transition dipole moment between the ground electronic states of the neutral OClO and its cation, which usually depends on the kinetic energy and the molecular geometry, but here is assumed to be a constant. E_0 is the energy of the vibrational ground level of the ground electronic state of the OClO molecule and $C'(t)$ is a damped time autocorrelation function of the wave packet evolving on the ionic electronic state. The autocorrelation function $C(t)$ is calculated by

$$C(t) = \langle|\Psi(t=0)|\mathrm{e}^{-i\hat{H}t}|\Psi(t=0)\rangle = \langle\Psi(0)|\Psi(t)\rangle = \left\langle\Psi\left(-\frac{t}{2}\right)\middle|\Psi\left(\frac{t}{2}\right)\right\rangle \quad (13)$$

We begin with a real wave packet $\Psi(t=0)$, and therefore, from a wave packet propagation time of $t/2$, we can obtain the

correlation function at time t.[32] $C'(t)$ is obtained by multiplying $C(t)$ with an exponential function

$$C'(t) = C(t)f(t) = C(t)\exp(-t/\tau) \tag{14}$$

This not only results in a smooth spectrum, but also convolutes the spectrum with a Lorentzian function of fwhm (full width at half-maximum) $\Gamma = 2/\tau$ which can be chosen to approximately reproduce the experimental broadening of the spectral peaks.

E. Potential Energy Surface for $OClO^+$. The OClO molecule plays an important role in the destruction of atmospheric ozone[33] and has an interesting phase-dependent photochemistry.[34] Therefore, a substantial amount of theoretical and experimental work has been devoted to the system.[33−47] An ab initio based three-dimensional potential energy surface of the ground state of the neutral OClO molecule has been reported by Peterson and Werner[35] and was used in our calculations. For the cation, we extend to three dimensions the two-dimensional MRCI potential energy surface of the ground electronic state of the cation reported by Peterson and Werner,[36] which was used in the work by Mok et al.[44] and Mahapatra et al.[45−47] For C_{2v} geometries, the potential energy surface of the cation has been fitted to a polynomial of the form

$$V(S_1,S_2) = \sum_{ij} C_{ij}(\Delta S_1)^i(\Delta S_2)^j \tag{15}$$

where S_1 is the symmetric stretch coordinate $(r_1 + r_2)/\sqrt{2}$ and S_2 the bending coordinate θ (r_1, r_2, and θ are the Eckart bond angle coordinates).

To obtain a three-dimensional potential energy surface for the cation ground electronic state, we first calculate the dimensionless normal coordinates of the ground electronic state of neutral OClO.[47] They are referred to as Q_{g1}, Q_{g2} and Q_u and describe the symmetric stretch, bending, and asymmetric stretch vibrations, respectively. These were calculated by the ***GF***-matrix method of Wilson et al.[48] using the experimentally deduced force field of Miyazaki et al.[49] and assuming a harmonic vibrational motion. The ***GF***-matrix method gives mass-weighted coordinates which are then transformed into the dimensionless normal coordinates by multiplying with $\omega_i^{1/2}$ (ω_i being the frequency of the ith vibrational mode, in atomic units). Then the dependence of the potential energy surface on the asymmetric stretch coordinate $S_3 = (r_1 - r_2)/\sqrt{2}$ is approximated by a harmonic potential $V(S_3) = k_u S_3^2/2 = \omega_u Q_u^2/2$. The parameter k_u is the force constant along the asymmetric stretch coordinate of the ground state of $OClO^+$ and ω_u is the harmonic frequency, for which we adopted the cation ab initio value of 1280 cm^{-1} reported by Alcamí et al.[50] Therefore, the potential energy surface used to model the cation ground state is expressed as

$$V(S_1,S_2,S_3) = \sum_{ij} C_{ij}(\Delta S_1)^i(\Delta S_2)^j + V(S_3) \tag{16}$$

Mahapatra and co-workers[45−47] used this method to extend other C_{2v} potential energy surfaces to three-dimensions in their calculations involving the neutral OClO and its anion and cation.

F. Numerical Parameters for the Wave Packet Calculations. In the calculations, the grid ranges are [1.6, 3.9] in atomic units for R_1 and R_2 and [1.9, 3.0] in radians for φ. We note that the equilibrium geometries of the OClO molecule and its cation are far from linear with deep bending wells. Therefore, we do not need to worry about the singularities of the Hamiltonian in eq 2. The grid numbers for R_1, R_2 and φ are 64, 64, and 32 respectively, which is enough to converge the calculations. The time step Δt used in the calculations is 0.25 fs.

III. Results and Discussion Application to OClO

Cornford et al. and Flesch et al. recorded the He I photoelectron spectrum of the OClO molecule.[43] The spectrum of Flesch et al., which has the better energy resolution, showed four distinct bands between 10 and 22 eV.[43] The first band is due to the ionization of the $3b_1$ unpaired electron of the OClO molecule which thereby forms the $^1A_1$ ground electronic state of the cation.[43] Two distinct vibrational progressions within this band were assigned to the symmetric stretch and bending vibrational modes of the cation $OClO^+$. The real time photodissociation dynamics of OClO has also been studied using the ultrashort pump−probe technique.[42] These experiments observed apparent biexponential decay after the pump excitation, but the explanations to this phenomenon vary.[42] Here we only report calculated He I photoelectron spectra, but first we discuss the accuracy of the eigenfunctions obtained by the 3D FGH method outlined above.

We note that ionizing an electron from the ground state of the OClO molecule to form $OClO^+$ in the ground state is a perpendicular transition. That means that the parity of the initial total wave function is opposite to that of the final wave function, which has been thoroughly discussed in ref 51. Even though the angular momentum changes during the excitation process, all results presented here are for a total angular momentum of zero.

A. Vibrational Eigenfunctions on the Fourier Grid. As mentioned, the potential energy surface of the ground electronic state employed in the calculation is the three-dimensional ab initio based surface reported by Peterson.[35] One-dimensional potential cuts along the variables R_1 (or R_2) and φ are shown in Figure 2. In each panel two coordinates are fixed at their equilibrium values. The figure indicates that only part of the angular φ range, 0 to π, is necessary to set up the grid. The lowest three eigenfunctions of the two (three) potential cuts are shown. The eigenvalues of the three-dimensional potential energy surface are found using a direct product basis of the one-dimensional eigenfunctions. Retaining the five lowest eigenfunctions along each degree of freedom in the direct product is enough to make the lowest vibrational level converge to within 0.01 cm^{-1}. Results for the two lowest eigenfunctions are listed in Table 1. These are compared with eigenvalues obtained using the Eckart bond Hamiltonian in ref 52 and expanding the wave function in a direct product basis of one-particle functions in Eckart bond coordinates[19]

$$\Psi(r_1,r_2,\theta) = \frac{1}{\sqrt{\sin\theta}} \sum_{n_{r_1},n_{r_2},n_\theta} C_{nr_1}C_{nr_2}C_{n\theta}\phi_{nr_1}(r_1)\phi_{nr_2}(r_2)\phi_{n\theta}(\theta) \tag{17}$$

where $\phi_{n_{ri}}(r_i)$ are Morse wave functions and $\phi_{n_\theta}(\theta)$ are harmonic oscillator wave functions. This method has been shown to give good convergence for the ground electronic state of the OClO molecule.[19]

From Table 1, we see that the three-dimensional Fourier grid Hamiltonian approach works well for obtaining the initial ground vibrational wave packet for the time-dependent calculation. The 3D FGH approach shows faster convergence than the Morse plus harmonic basis functions method as a function of basis size, in the present application. We however note the difference in absolute values between the eigenvalues obtained from the Morse plus harmonic basis functions and the corresponding

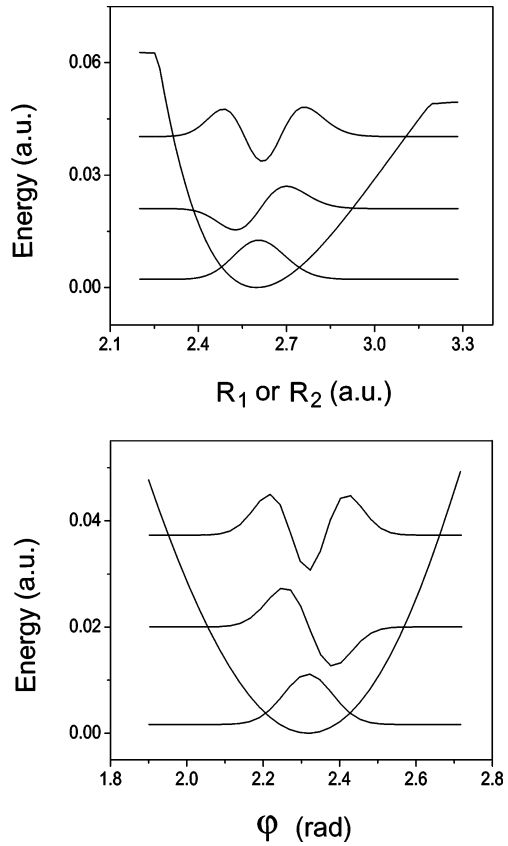

Figure 2. One-dimensional cuts through the ground-state OClO potential energy surface along the variables R_1 (or R_2) and φ in Radau coordinates. In each panel, two coordinates are at their equilibrium values. The first three eigenfunctions for each potential curve are found by the one-dimensional Fourier grid Hamiltonian method and shown in the figure. There are 64 grid points along R_1 (or R_2) and 32 along φ.

TABLE 1: The Two Lowest Eigenvalues[a] of OClO on the Three-Dimensional Potential Energy Surface of Peterson[35]

	no. of eigenfunctions[b,c]	method A	method B	method C
(0,0,0)	(4,4,4)	1264.2251	1264.0866	1264.3326
	(5,5,5)	1264.1857	1263.9700	1264.2153
	(6,6,6)	1264.1795	1263.9416	1264.1867
	(7,7,7)	1264.1784	1263.9357	1264.1807
	(9,9,9)	1264.1782	1263.9336	1264.1785
(0,1,0)	(4,4,4)	1714.9111	1714.4980	1714.8325
	(5,5,5)	1714.2251	1713.9174	1714.3053
	(6,6,6)	1714.1322	1713.8146	1714.1482
	(7,7,7)	1714.1177	1713.7863	1714.1199
	(9,9,9)	1714.1144	1713.7812	1714.1147

[a] The eigenvalues are obtained by the three-dimensional Fourier grid Hamiltonian method (A) or using Morse plus harmonic basis functions (B). In method C, the wave function obtained by method B is transformed to Radau coordinates and the energy is then obtained as $\langle\Psi|H|\Psi\rangle$ where H is the Fourier grid Hamiltonian in Radau coordinates. The zero of energy is at the classical minimum of the potential. [b] The first two numbers are the number of the basis functions along the variables R_1 and R_2 in Radau coordinates or r_1 and r_2 in bond bond-angle coordinates. The third number is the number of basis functions in the angular coordinate. [c] For method A, the one-dimensional basis sets along each coordinate are converged, and the numbers indicate how many eigenfunctions are kept in each coordinate for forming the direct product basis.

energies obtained using the 3D FGH method. This results from the two different Hamiltonians and the numerical methods used.

Employing the widely used Hamiltonian in bond bond-angle coordinates[19,52] and proceeding as in ref 19, the Hamiltonian matrix constructed from the basis functions in eq 17 becomes nonhermitian. As a result, the eigenenergies are different from those obtained by the 3D FGH method. This is further illustrated by the last column in Table 1. There the wave function Ψ, obtained using the Eckart bond Hamiltonian with Morse plus harmonic basis functions, is expressed in Radau coordinates and the energy is then obtained as $\langle\Psi|H|\Psi\rangle$ where H is the Hamiltonian in Radau coordinates. It is clear that the eigenenergies now are larger than for the 3D FGH approach but converge toward the same value as the basis set size increases.

The influence of the nonhermiticity of the Eckart bond Hamiltonian matrix on the lowest vibrational level is rather small. The nonhermiticity of the Hamiltonian matrix has somewhat stronger impact on the higher vibrational level in Table 1, and this is expected to get worse as still higher levels are studied.

B. The First Band of the He I Photoelectron Spectrum of OClO. Mok et al.[44] have carried out an anharmonic Franck−Condon simulation of the He I photoelectron spectroscopy of the OClO molecule using the three-dimensional ab initio potential energy surface of Peterson[35] for the ground state of the neutral OClO molecule and the two-dimensional ab initio potential energy surface of Peterson and Werner[36] for the ground state of the cation. They however modified the potential energy surface of the neutral OClO to have the experimental equilibrium geometry. Thus, in their iterative Franck−Condon analysis Mok et al.[44] could derive a corresponding "experimental" equilibrium geometry of the cation ground state.

Using a two-dimensional time-dependent wave packet method in Jacobi coordinates, Mahapatra and Krishnan[45] produced the experimental He I photoelectron spectrum[43] in the first band. They employed the two-dimensional ab initio C_{2v} potential energy surfaces of Peterson and Werner[36] and found an intensity maximum at the photoelectron spectrum band origin in contrast to the experiments. By instead using the modified cationic surface derived by Mok et al., they obtained better agreement with the experimental spectrum. The reduced dimensionality results of Mok et al.[44] and Mahapatra and Krishnan[45] suggested that the asymmetric stretch plays only a marginal role in the electronic transition process.

Below we use the three-dimensional wave packet method in Radau coordinates and the potential energy surfaces specified in section II to calculate the first band of the photoelectron spectrum of OClO. In agreement with the reduced dimensionality simulations,[45] we find that the asymmetric stretch is not active in the transition process. Our calculated spectra agree better with the experimental spectrum using the improved cation equilibrium geometry of Mok et al. than using the equilibrium geometry of the original ab initio potential energy surface. However, our full dimensional calculation using the ab initio equilibrium geometry of the cationic ground state does not lead to a maximum at the band origin, in contrast to the two-dimensional work of Mahapatra and Krishnan. This is discussed below as is a small modification to the equilibrium geometry of Mok et al. which further improves the reproduction of the experimental photoelectron spectrum.

Our computed results using the 3D wave packet method and the ab initio potential energy surfaces of Peterson and Werner,[35,36] with the extension to 3D for the cationic surface, are shown in the upper panel of Figure 3. We have set the adiabatic ionization energy (AIE) to 10.33 eV, which is higher than the ab initio value by about 0.1 eV. The adjustment of the AIE is necessary to correctly reproduce the locations of the spectral peaks. This is consistent with the results of Mahapatra and Krishnan.[45] The spectrum clearly shows two different vibrational

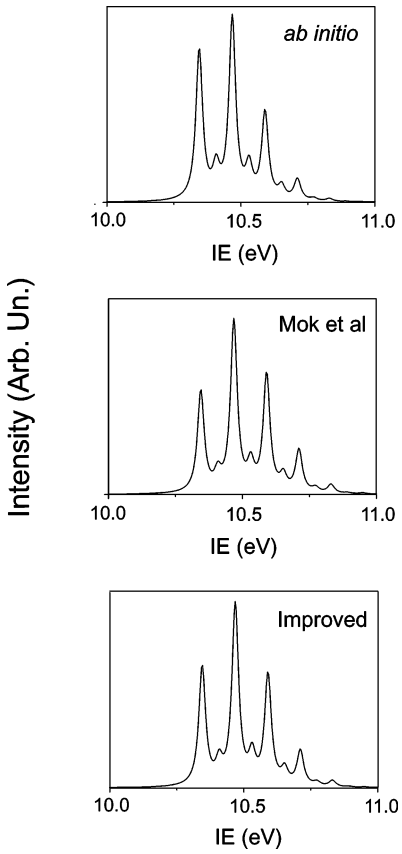

Figure 3. Calculated first photoelectron band of the OClO molecule. Upper panel: using the ab initio equilibrium geometry of the cationic ground state. Middle panel: using the improved equilibrium geometry derived by Franck−Condon analysis.[44] Bottom panel: using the parameters listed in Table 2. The bottom spectrum reproduces the experimental spectrum best. Before Fourier transformation, the time autocorrelation function has been exponentially damped with a parameter value which is equivalent to convoluting the spectrum with a Lorentzian function with fwhm of 30 meV.

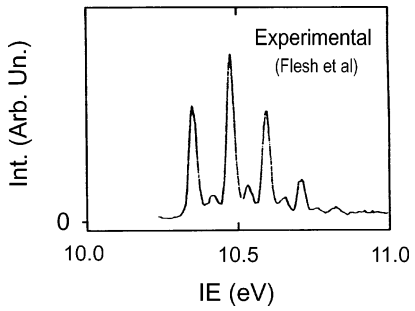

Figure 4. Experimental first photoelectron band of the OClO molecule. Reprinted from the work of Flesch et al.[43] Copyright 1971 American Chemical Society.

progressions, a quite strong progression along the symmetric stretch and a relatively weak one along the bending mode, in agreement with the experimental observation; see Figure 4. The energy distances between the peaks of the two progressions are 125 and 66 meV, corresponding respectively to the symmetric stretch and bending vibrational frequencies of the ground electronic state of $OClO^+$.

The maximum of the band in the upper panel in Figure 3 does not appear at the band origin, but at the second peak, which is different from the results of the two-dimensional work of Mahapatra and Krishnan[45] where the maximum appears at the band origin. This may result from the difference between the equilibrium geometries of the ground electronic state of the neutral OClO molecule of the different ab initio works which are used in the polynomial expansion of the corresponding potential energy surface. In our calculation, the three-dimensional ab initio surface of Peterson is used,[35] while in the work of Mahapatra and Krishnan, the earlier two-dimensional surface reported by Peterson and Werner was used.[36]

TABLE 2: Improved Parameters for the Cation Ground Electronic State

r_e (au)	θ_e (deg)	T_e (eV)
2.678	121.8	10.33

Our calculated results using the equilibrium geometry of Mok et al. for the cation[44] are depicted in the middle panel of Figure 3. This equilibrium geometry gives results in better agreement with the experiment than that of the ab initio work;[36] compare this to Figure 4 where the first photoelectron band of Flesch et al.[43] is reproduced. The third peak of the symmetric stretch progression is a little larger, but the first peak of the same progression is a little smaller, compared to the results of the experiment of Flesch et al.[43] and the anharmonic Franck−Condon calculations.[44]

In the anharmonic Franck−Condon work of Mok et al.,[44] the 2D ab initio potential energy surface for the cation[36] and the 3D ab initio potential energy surface[35] for neutral OClO were used, but for neutral OClO the equilibrium geometry was modified as stated above. The overall shape of the spectrum sensitively depends on the relative equilibrium geometries of the ground electronic states of the neutral OClO and its cation. Therefore, the equilibrium geometry of the cation derived by Mok et al.[44] does not work perfectly together with the ab initio equilibrium geometry for the neutral OClO molecule. Here we assume that the ab initio equilibrium geometry of the three-dimensional potential energy surface of the neutral molecule has been obtained accurately and optimize the equilibrium geometry of the cationic ground state by iteratively comparing with the experimental photoelectron spectrum.

We find that by using $r_e = 2.678$ au and $\theta_e = 121.8°$ in the polynomial expansion of the potential energy surface of the cation, a spectrum in good agreement with the experimental observation is obtained. Compared with the parameters $r_e = 2.672$ au and $\theta_e = 121.8°$ of Mok et al.,[42] the value of r_e has been increased by 0.006 au. The original ab initio values[36] were $r_e = 2.6897$ au and $\theta_e = 120.78°$. The spectrum corresponding to the new equilibrium geometry of the cation is shown in the bottom panel of Figure 3, which can be compared with the experimental photoelectron spectrum in Figure 4. There is clear improvement using the parameters of our modified equilibrium geometry. In Table 2, we summarize the parameters in the polynomial expansion of the potential energy surface for the cationic ground electronic state which we found to best reproduce the experimental photoelectron spectrum. The numerically calculated absorption spectrum is quite sensitive to the parameters in Table 2, so the new values are significantly different from those of Mok et al. However, the accuracy of our modified equilibrium geometry depends on the quality of the used potential energy surfaces and the approximation that the OClO molecule does not rotate.

IV. Summary

In this work, we introduce a three-dimensional time-dependent wave packet method in Radau coordinates based on the Fourier grid Hamiltonian method. The fast Fourier transform is used in all degrees of freedom to realize the actions of the kinetic energy operators on the wave packet. The propagation

is performed by the second order split operator method for a total angular momentum of zero. The triatomic Hamiltonian in Radau coordinates is identical in form with that in Jacobi coordinate, but snapshots of the wave packet in Radau coordinates can be approximately interpreted as bond bond-angle (Eckart bond) coordinates. This aspect is of particular interest in simulating real-time pump−probe experiments. We can alternatively calculate the dynamics in Eckart bond coordinates, but this involves more operators and therefore more computational time. Because of the similarity of the Jacobi and Radau Hamiltonians of triatomic systems, the code based upon the method introduced here can easily be adopted to study systems which are better described in Jacobi coordinates.

To calculate the photoelectron spectrum, we first find the lowest vibrational eigenfunction of the ground electronic state of the neutral nonrotating OClO molecule. This is done by using a direct product of one-dimensional eigenfunctions found by applying the Fourier grid Hamiltonian method of Marston and Balint-Kurti[20] to each of the three Radau coordinates in turn, keeping the other two fixed at their equilibrium values. The potential energy surface used in the calculation is the three-dimensional one reported by Peterson.[35] Comparing the eigenvalues obtained in this way with results from Morse plus harmonic basis function calculations, we found that the presented method works well.

The wave function obtained for the ground vibrational level is used as the initial wave function and propagated on the ground electronic state of the cation. The autocorrelation function is obtained and Fourier transformed to give the first band of the photoelectron spectrum of the OClO molecule. In the calculation, the two-dimensional potential energy surface of the cationic ground electronic state of Peterson and Werner[36] has been extended to a three-dimensional one by assuming a harmonic asymmetric stretch. The spectrum obtained from the three-dimensional calculation is similar to that of a previous two-dimensional model[45] and an anharmonic Franck−Condon calculation.[44] In all cases the asymmetric stretch is inactive in the ionization transition.

Assuming that the three-dimensional potential energy surface of the ground electronic state of the OClO molecule is accurate, we modified three parameters for the potential energy surface of the cationic ground electronic state in order to obtain improved agreement between the calculated and experimental photoelectron spectrum. The parameters are given in Table 2.

Acknowledgment. Z.S. is grateful to Professor S. Mahapatra for helpful communications. This work is supported by the National Science Foundation (No. 29833080), the Knowledge Innovation Program of the Chinese Academy of Science Grant and the Science Research Council of Sweden.

References and Notes

(1) Kosloff, R. *J. Phys. Chem.* **1988**, *92*, 2087.
(2) Meier, Ch.; Engel, V. *Chem. Phys. Lett.* **1992**, *200*, 488.
(3) Heitz, M.-C.; Durand, G.; Spiegelman, F.; Meier, Ch. *J. Chem. Phys.* **2003**, *118*, 1282.
(4) Sun, Z.; Lou, N. *Phys. Rev. Lett.* **2003**, *91*, 023002.
(5) González, L.; Hoki, K.; Kröner, D.; Leal, A. S.; Manz, J.; Ohtsuki, Y. *J. Chem. Phys.* **2000**, *113*, 11134.
(6) Sola, I. R.; Santamaria, J.; Tannor, D. J. *J. Phys. Chem.* **1998**, *102*, 4301.
(7) Nyman, G.; Yu, H.-G. *Rep. Prog. Phys.* **2000**, *63*, 1001.
(8) Katz, G.; Yamashita, K.; Zeiri, Y.; Kosloff, R. *J. Chem. Phys.* **2002**, *116*, 4403.
(9) Barinovs, Ğ.; Markovic, N.; Nyman, G. *Chem. Phys. Lett.* **1999**, *315*, 282.
(10) Füsti-Molnár, L.; Szalay, P. G.; Balint-Kurti, G. G. *J. Chem. Phys.* **1999**, *110*, 8448.
(11) Radau, R. *Ann. École Normale Supérior* **1868**, *5*, 311.
(12) Adamov, M. N.; Natanson, G. A. *Vestn. Leningr. Univ.* **1973**, *4*, 28.
(13) Smith, F. T. *Phys. Rev. Lett.* **1980**, *45*, 1157.
(14) Möbius, P. *Nucl. Phys.* **1960**, *16*, 278; *Nucl. Phys.* **1960**, *18*, 224; *Nucl. Phys.* **1961**, *28*, 304.
(15) Johnson, B. R.; Reinhardt, W. P. *J. Chem. Phys.* **1986**, *85*, 4538.
(16) Sutcliffe, B. T.; Tennyson, J. *Int. J. Quantum Chem.* **1991**, *39*, 183. The definition of the Radau coordinates used in this reference is different from the traditional form, which is used in the present work.
(17) Sutcliffe, B. T.; Tennyson, J. *Mol. Phys.* **1986**, *58*, 1053.
(18) Barinovs, Ğ.; Markovic, N.; Nyman, G. *J. Phys. Chem.* **2001**, *105*, 7441.
(19) Barinovs, Ğ.; Markovic, N.; Nyman, G. *J. Chem. Phys.* **1999**, *111*, 6705.
(20) Marston, C. C.; Balint-Kurti, G. G. *J. Chem. Phys.* **1989**, *91*, 3571.
(21) Balint-Kurti, G. G.; Ward, C. L.; Marston, C. C. *Compt. Phys. Commun.* **1991**, *67*, 285.
(22) Light, J. C.; Hamilton, I. P.; Lill, J. V. *J. Chem. Phys.* **1985**, *82*, 1400.
(23) Baye, D.; Heenen, P.-H. *J. Phys. A: Math. Gen.* **1986**, *19*, 2041.
(24) Harris, D. O.; Engerholm, G. G.; Gwinn, W. D. *J. Chem. Phys.* **1965**, *43*, 1515.
(25) Dickinson, A. S.; Certain, P. R. *J. Chem. Phys.* **1969**, *49*, 4209.
(26) Greenawalt, E. M.; Dickinson, A. S. *J. Mol. Spectrosc.* **1969**, *30*, 427.
(27) Semay, C. *Phys. Rev. E* **2000**, *62*, 8777.
(28) Feit, M. D.; Fleck, J. A., Jr. *J. Chem. Phys.* **1983**, *78*, 301.
(29) Feit, M. D.; Fleck, J. A., Jr.; Steiger, A. *J. Comput. Phys.* **1982**, *47*, 412.
(30) Eno, L. *J. Chem. Phys.* **2000**, *113*, 453.
(31) Heller, E. J. *Acc. Chem. Res.* **1981**, *14*, 368.
(32) Engel, V. *Chem. Phys. Lett.* **1992**, *189*, 76. Manthe, U.; Meyer, H.-D.; Cederbaum, L. S. *J. Chem. Phys.* **1992**, *97*, 9062.
(33) Vaida, V.; Simon, J. D. *Science* **1995**, *268*, 1443.
(34) Reid, P. J. *J. Phys. Chem.* **2002**, *106*, 1473.
(35) Peterson, K. A. *J. Chem. Phys.* **1998**, *109*, 8864.
(36) Peterson, K. A.; Werner, H.-J. *J. Chem. Phys.* **1992**, *96*, 8948.; Peterson, K. A.; Werner, H.-J. *ibid* **1993**, *99*, 302.
(37) Richard, E. C.; Vaida, V. *J. Chem. Phys.* **1991**, *94*, 163. Richard, E. C.; Vaida, V. *J. Chem. Phys.* **1990**, *94*, 153.
(38) Sun, Z.; Lou, N.; Nyman, G. *Chem. Phys.*, in press.
(39) Esposito, A. P.; Stedl, T. Jónsson, H.; Reid, P. J.; Peterson, K. A. *J. Chem. Phys.* **1999**, *103*, 1748.
(40) Hubinger, S.; Nee, J. B. *Chem. Phys.* **1994**, *181*, 247. Marston, G.; Walker, I. C.; Mason, N. J.; Gingell, J. M.; Zhao, H.; Brown, K. L.; Motte-Tollet, F.; Delwiche, J.; Siggel, M. R. F. *J. Phys. B: At. Mol. Opt. Phys.* **1998**, *31*, 3387.
(41) Davis, H. F.; Lee, Y. T. *J. Chem. Phys.* **1996**, *105*, 8142. Furlan, A.; Scheld, H. A.; Huber, J. R. *J. Chem. Phys.* **1997**, *106*, 6538. Delmdahl, R. F.; Bakker, B. L. G.; Parker, D. H. *J. Chem. Phys.* **2000**, *112*, 5298.
(42) Baumert, T.; Herek, J. L.; Zewail, A. H. *J. Chem. Phys.* **1993**, *99*, 4430. Ludowise, P.; Blackwell, M.; Chen, Y. *Chem. Phys. Lett.* **1997**, *273*, 211. Blackwell, M.; Ludowise, P.; Chen, Y. *J. Chem. Phys.* **1997**, *107*, 283. Stert, V.; Ritze, H.-H.; Nibbering, E. T. J.; Radloff, W. *Chem. Phys.* **2001**, *272*, 99.
(43) Cornford, A. B.; Frost, D. C.; Herring, F. G.; McDowell, C. A. *Chem. Phys. Lett.* **1971**, *10*, 345. Cornford, A. B.; Frost, D. C.; Herring, F. G.; McDowell, C. A. *Faraday Discuss. Chem. Soc.* **1972**, *54*, 56. Flesch, R.; Ruhl, E.; Hottmann, K.; Baumgartel, H. *J. Phys. Chem.* **1993**, *97*, 837.
(44) Mok, K. W.; Lee, P. F.; Chau, F. T.; Wang, D.; Dyke, J. M. *J. Chem. Phys.* **2000**, *113*, 5791.
(45) Mahapatra, S.; Krishnan, G. M. *J. Chem. Phys.* **2001**, *115*, 6951.
(46) Krishnan, G. M.; Mahapatra, S. *J. Chem. Phys.* **2003**, *118*, 8715.
(47) Mahapatra, S.; Ritschel, T. *Chem. Phys.* **2003**, *289*, 291.
(48) Wilson, Jr., E. B.; Decius, J. C.; Cross, P. C. *Molecular Vibrations*; McGraw-Hill: New York, 1955.
(49) Miyazaki, K.; Tanoura, M.; Tanaka, K.; Tanaka, T. *J. Mol. Spectrosc.* **1986**, *116*, 435.
(50) Alcamí, M.; Mó, O.; Yáñez, M.; Cooper, I. L. *J. Phys. Chem. A* **1999**, *103*, 2793.
(51) Balint-Kurti, G. G.; Füsti-Molnár, L.; Brown, A. *Phys. Chem. Chem. Phys.* **2001**, *3*, 702.
(52) Carter, S.; Handy, N. C. *Mol. Phys.* **1986**, *57*, 175.